Thermal Durability Characterization of a Simple Polymethyl-methacrylate (PMMA) Based-Optical Waveguide

Ian Yulianti [1,a,*], Shiva Maulana Khoiru Insan [1,b], Ngurah Made Darma Putra [1,c], Aji Purwinarko [1,d] , Nuni Widiarti [1,e], and Nor Hafizah Ngajikin [2,f]

[1] Department of Physics, Faculty of Mathematics and Natural Sciences, Universitas Negeri Semarang, Sekaran, Gunungpati, Semarang, Indonesia
[2] Faculty of Electrical and Electronics, Universiti Tun Hussein Onn, Batu Pahat, Johor Bahru, Malaysia

e-mail: [a] ianyulianti@mail.unnes.ac.id, [b] shivamaulana1@gmail.com, [c] ngurahmade.dp@mail.unnes.ac.id, [d] aji.purwinarko@mail.unnes.ac.id, [e] nuni_kimia@mail.unnes.ac.id, and [f] norhafizah@uthm.edu.my
* Corresponding Author

Received: 26 January 2024; Revised: 29 July 2024; Accepted: 12 September 2024

Abstract

Polymethyl-methacrylate (PMMA)-based optical waveguide is a good candidate for a simple and low-cost waveguide. However, the thermal properties have not been explored. The purpose of the work is to investigate the thermal properties of PMMA-based waveguide. Waveguide fabrication process was done in three stages, which are patterning the PMMA cladding, core material synthetization and core material application to the cladding. Core pattern with cross section area of 1×1 mm² was engraved on the 4 cm long PMMA sheet. Unsaturated polyester resin (UPR) was used as a core material. Characterizations were conducted for temperature dependent loss (TDL), temperature working range, and long exposure durability. For TDL characterization, the temperature varied from 30°C to 75°C. Meanwhile, for temperature working range, the waveguide was exposed to cycled heating. The thermal durability characterization was done by immersing the waveguide in distilled water at temperature of 40 °C for 288 hours. The results showed that a little change of output intensity occurred due to temperature variation with TDL of 0.0235 dB/°C. The maximum limit of the temperature is 70°C. For long exposure to temperature of 40°C, the results showed that the waveguide has a good performance. It can be concluded that, for temperatures below 70°C, the waveguide performance is not strongly affected by environmental temperature. Further research is required to enhance its thermal stability and to further reduce temperature sensitivity.

Keywords: *Waveguide; Polymethyl-methacrylate (PMMA); Unsaturated polyester resin (UPR); thermal durability*

How to cite: Yulianti I, Insan SMK, Putra NMD, Purwinarko A, Widiarti N, and Ngajikin NH**.** Thermal Durability Characterization of a Simple Polymethyl-methacrylate (PMMA) Based-Optical Waveguide. *Jurnal Penelitian Fisika dan Aplikasinya (JPFA)*. 2024; 14(2): 113-124. DOI: https://doi.org/10.26740/jpfa.v14n2.p113-124.

© 2024 Jurnal Penelitian Fisika dan Aplikasinya (JPFA). This work is licensed under CC BY-NC 4.0

INTRODUCTION

Optical waveguide has been widely used in optical telecommunication and optical sensors due to its advantages such as immune to electromagnetic interference, suitable for hazardous environment, high resistance to bending, compact, reliable, and can be integrated in optical integrated circuit [1]. In optical telecommunications, waveguides can be found in various applications such as division multiplexer [2], [3], optical splitter [4]–[6], and optical switch [7]–[9]. In optical sensor applications, waveguide has been used for gas detection [10], [11], temperature sensor [12], and biosensor [13], [14].

Despite its numerous advantages, waveguides also have certain limitations such as fabrication complexity. The fabrication of optical waveguides can be complex and require specialized techniques such as lithography [15], [16], etching [17], laser writing [18], deposition [19] and three-dimensional microfabrication technique [20]. Complex fabrication techniques are costly and time-consuming which limits the scalability and cost-effectiveness of waveguide-based technologies. Moreover, optical waveguides can be sensitive to external factors such as temperature. Due to thermo-optic effect, variations in temperature cause the change in refractive index of the waveguide material which affects the light propagation. Therefore, it may result in signal distortion and performance degradation.

A simple fabrication method was proposed by Hamid et.al [21] which used Polymethyl Methacrylate (PMMA) and polyvinyl chloride as waveguide material. A groove with 0.6 ×0.6 mm^2 cross sectional area was made on the PMMA sheet and then filled with photo-resist epoxy resin. Characterization results showed that the waveguide has propagation loss of 2.54 dB/cm at wavelengths of 1550 nm and 1310 nm. Other simple waveguide fabrication technique has been proposed by using hot embossing technique with PMMA as the waveguide material [22],[23]. The waveguide was fabricated by pressing a structured stamp on a heated PMMA sheet at a temperature of 140^{o}C. The PMMA waveguides have dimensions of H100 ⌈m and work at wavelength of 850nm for carbon diode sensor application.

Another candidate for a simple and low-cost waveguide has been proposed using PMMA as cladding and Unsaturated Polyester Resin (UPR) as core material [24]. UPR material was used since it has a higher refractive index value than PMMA. The waveguide was fabricated by engraving the PMMA using Computer Numerical Control (CNC) engraving machine to make a pattern of the core structure forming a trench. The trench with a cross section of 1×1 mm^2 was then filled with UPR solution. The result showed that power loss is -7.89 dB. The waveguide has a good potential for measurement of liquid refractive index since it uses visible light as the source which minimize the absorption loss [25]. Characterization showed that the waveguide has sensitivity to Refractive Index (RI) as high as -48.476 dB/Refractive Index Unit (RIU).

However, previous research has not specifically explored the combination of PMMA and UPR in the context of the thermal stability of optical waveguides. Furthermore, detailed TDL characterization and long-term thermal exposure tests across varying temperatures have not been extensively covered. Existing studies have primarily focused on individual materials and different fabrication methods, lacking the comprehensive approach taken in this research. Investigating the thermal stability of waveguide is important since temperature might affect the waveguide characteristics because of the thermo-optic nature.

In general, waveguides can work well at temperatures up to 85°C. However, after a certain period of exposure to this temperature, the waveguides might experience attenuation. Some waveguides can maintain their performance at 85 °C for up to 5000 hours of usage, while some others can withstand to temperature of 90 °C and are still stable after 600-700 hours of usage. Günther, et al. [26] examined the effect of temperature on self-written waveguides (SWW) made of polymer which were connected using a low-loss coupling structure and applied to the self-writing process. The results show that SWW can be used as a sensor element capable of detecting temperatures of ±5°C. However, when the waveguide was exposed to temperature of 60°C, the output intensity decreased. Therefore, it is important to investigate the effect of temperature on PMMA waveguide performance as a candidate of a low cost and simple fabricated waveguide. This study performs a comprehensive characterization of the thermal performance of this waveguide, including measurements of temperature-dependent loss (TDL), operational temperature range, and long-term thermal exposure.

METHOD

Fabrication

Waveguide fabrication process was done in three stages, which are patterning the PMMA cladding, core material synthetization and core material application to the cladding. PMMA sheet with thickness of 2 mm and area of 4 × 2 cm^2 was used as the cladding. The PMMA was then carved using a CNC machine forming a straight trench with cross section area of 1 × 1 mm^2. At both ends of the trench, a plastic optical fiber (POF) with a length of 17 cm was attached to the PMMA. The waveguide structure prior to application of upper cladding is depicted in Figure 1.

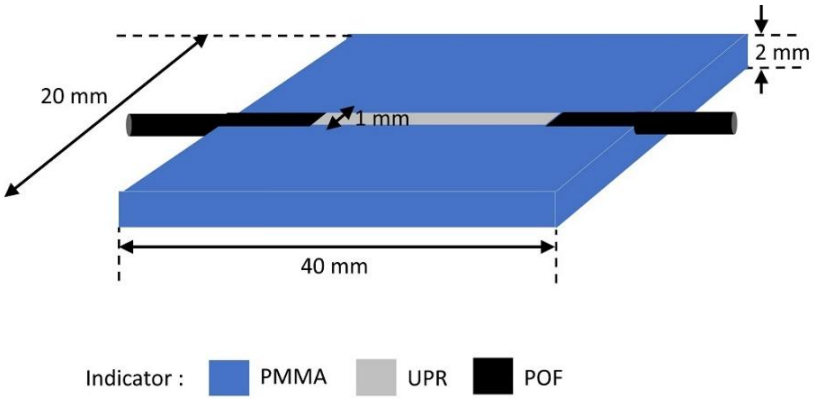


Figure 1. Waveguide Structure Without Upper Cladding

Core material synthetization was done by mixing the UPR with Methyl Ethyl Ketone Peroxide (Mepoxe) as a crosslinking agent with ratio of 400:1. The UPR solution was stirred using magnetic stirrer at 60 rpm at room temperature until the UPR is perfectly dissolved. The stirring was done slowly to avoid bubbles that might occur due to the stirring process. The presence of bubbles could cause propagation loss thereby reducing the performance of the waveguide.

The final fabrication step is filling the trench on the PMMA sheet with UPR solution. UPR was poured slowly and gradually to avoid the formation of bubbles in the waveguide core. The residue that was formed on top of the UPR layer was cleaned immediately before the solution hardened using optical fiber sandpaper. The UPR was cured at room temperature for 24 hours. After the UPR had hardened, the surface was smoothed using a cutter and P60 sandpaper. Then the sample was re-sanded using acetone to flatten the surface before covering the top with un-graved PMMA sheet which functions as the top cladding of the waveguide.

Characterizations

The characterization was carried out for TDL, the temperature working range, and the long exposure durability. To provide uniform heat distribution along the waveguide, temperature exposure was done in the heated distilled water. For TDL characterization, the temperature varied from 30°C to 75°C. The input port of the waveguide was connected to a red LED with a wavelength of 660 nm. The other end of the waveguide was connected to a photodiode and multimeter, as shown in Figure 2.

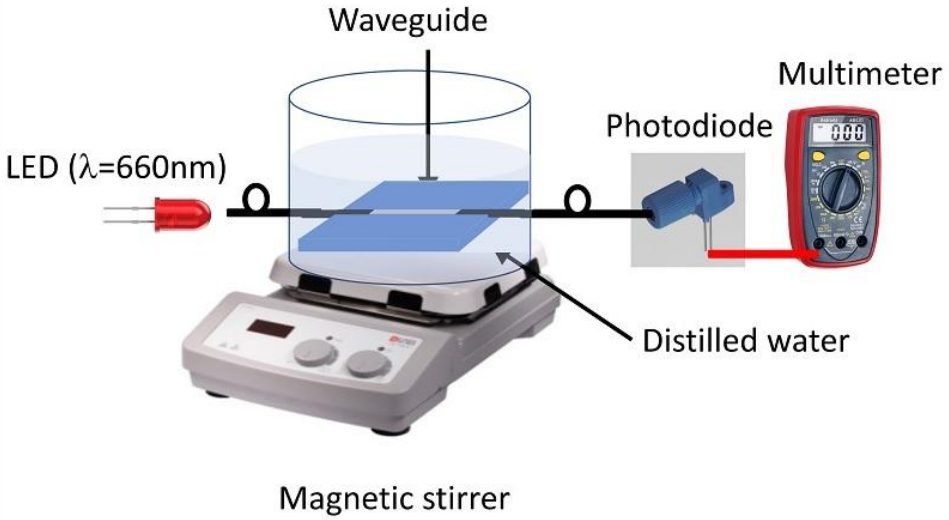


Figure 2. Characterization Set Up for TDL, Temperature Working Range and The High Temperature-Long Exposure Effect

By recording the input and output voltage, the power loss (L) was obtained by using equation (1)

$$L\,(dB) = \left|20\ log\ log\ \frac{Vout}{Vin}\right| \quad (1)$$

where V_{in} is the input voltage, and V_{out} is the output voltage. For each temperature value, the output voltage was recorded every ten 30 seconds until the value was stable, indicating that it had reached the equilibrium state.

For the temperature working range characterization, the waveguide was exposed to cycled heating. The temperature was raised up to the test temperature and then the temperature was decreased back to the room temperature (25°C). The cycle was repeated for six test temperatures namely 30 °C, 40 °C, 50 °C, 60 °C, 70 °C and 80 °C. Prior to the cycled heating, the loss at room temperature was first measured to determine the initial loss (L_i). The loss at room temperature of each cycle is defined as the return loss (L_r). The upper limits of the temperature working range is defined as the maximum temperature before L_r is significantly deviated from L_i which is indicated by high $\otimes L$, where

$$L = L_{r_}L_i. \quad (2)$$

The thermal durability characterization was done by immersing the waveguide in distilled water at temperature of 40 °C for 288 hours. Temperature of 40°C was chosen since it is the highest possible environmental temperature. The output voltage was recorded every 24 hours. The waveguide performance was analyzed by plotting the loss vs exposure time. The maximum exposure time is defined as the maximum duration at which the power loss is maintained by investigating the loss performance. To further analyze the temperature effect to the core material, the surface morphology and chemical content of the UPR was observed using SEM/EDX prior and after the heating.

RESULTS AND DISCUSSION

Prior to the characterization stage, the fabricated waveguide profile was observed using a charged-coupled device (CCD) microscope. The image obtained from the microscope is shown in Figure 3.

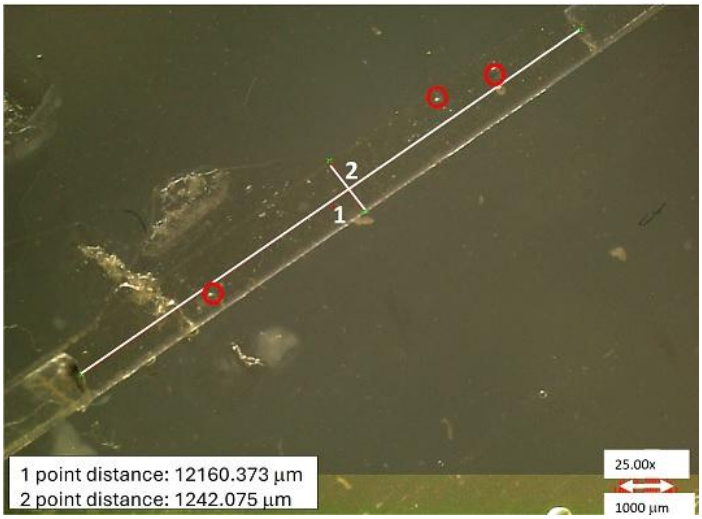


Figure 3. CCD Microscope Image of The UPR based Waveguide. Some Bubbles Were Formed in The Core and Outside Core Area

As shown in Figure 3, it is observed that there is some dirt and a few bubbles observed outside the waveguide core (signed by the red circles). The dirt might be exhibited from excess dust and other residual particles which dissolved during the stirring process which were not completely removed. Bubbles introduce discontinuities in the refractive index profile of the waveguide. This mismatch in refractive index can cause reflection and scattering at the bubble interface, leading to insertion losses.

Based on thermal properties of the POF which has an operating temperature up to 85°C, the TDL characterization was done for the temperature range from room temperature at 25°C to 80°C. The TDL was obtained by plotting the power loss vs temperature, as shown in Figure 4.

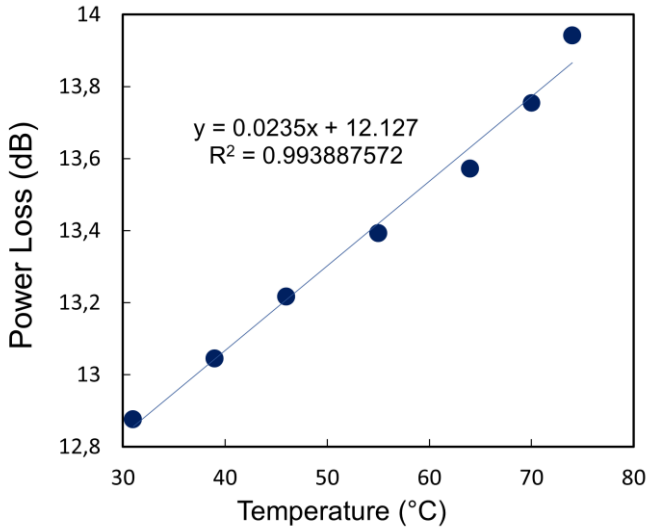


Figure 4. Power Loss vs. Temperature of the PMMA Based Waveguide. The TDL is Defined as The Slope of The Graph**.**

As shown in Figure 4, the power loss in an UPR waveguide increases linearly with temperature, with TDL of 0.0235 dB/°C. The value is comparable to that of bending plastic optical fiber which is 0.011dB/°C [27]. However, the results were also affected by the fluctuation of the environment temperature since the characterization set up was not isolated. Therefore, the TDL value might decrease if the characterization is conducted in isolated system. The increase of power loss is due to the decrease in the refractive index of the core as the temperature increases as the effect of the negative thermo-optic coefficient. The refractive index of the core is what determines the numerical aperture (NA) of the waveguide, and a lower NA means that fewer modes of light can be transmitted, resulting in higher power loss [28]. For temperature working range characterization, the results are shown in Figure 5.

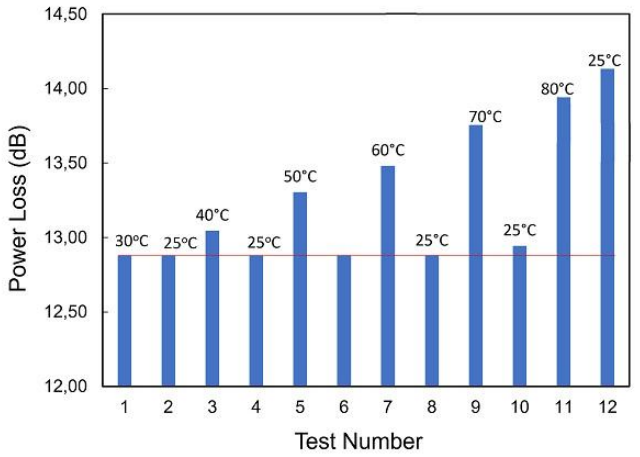


Figure 5. Power Loss of Waveguide Obtained During Cycled Heating Exposure to Determine the Temperature Working Range

For temperature working range characterization, the results showed that the initial power loss at room temperature (L_i) is 12.88 dB, as shown in Figure 5. When the waveguide was exposed to cycled heating up to 70°C, it was shown that, at each cycle, L_s were ±0.06 dB. However, when the temperature was increased to 80°C and then decreased back to room temperature, the results showed that there was a significant increase in power loss. Therefore, the upper limit of temperature working range of the waveguide is 70°C.

Waveguide that was damaged due to exposure to high temperature, was observed using Scanning Electron Microscope (SEM) to observe the surface profile and the chemical contents. The SEM image before and after high temperature exposure are shown in Figure 6.

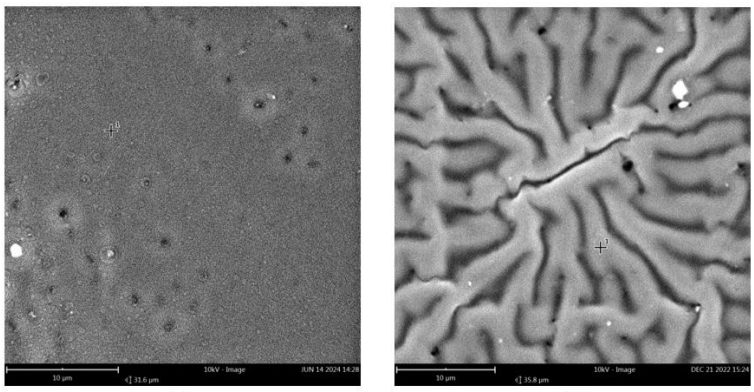


Figure 6. SEM image of waveguide core surface (a) before heated and (b) after heated up to 80°C

Prior heating, the surface of the waveguide core is notably smooth and homogeneous, and planarity as shown in Figure 6(a). There are no visible defects, cracks, or irregularities on the surface which is characteristic of glassy materials[29]. The results agree well with that obtained by Salemane et.al. [29-30]. Post-heating, the surface exhibits increased roughness, as shown in Figure 6(b). This roughness can result from thermal expansion and contraction cycles that induce stress within the material, potentially leading to surface deformation. There are indications of microcracks or fissures, which are typical signs of thermal fatigue. These microcracks can propagate under continuous thermal cycling, compromising the structural integrity of the waveguide. The surface changes suggest that the material may be undergoing thermal degradation. At 80°C, polymers or composite materials commonly used in waveguides might start to exhibit signs of degradation, such as discoloration or a change in texture. When heated, the UPR experiences mass loss which further results in decreased density [31-32]. The mass decreased at a slow and steady rate as the temperature increased [33]. Moreover, the waveguide also experienced thermal expansion when exposed to heat [34]. When the temperature was decreased back to room temperature, the material was shrinking back. However, due to the mass loss while heated, the core surface was no longer homogenous as shown in Figure 6 (b). The core surface has been deformed and wrinkled**.** For chemicals content of the heated waveguide, EDX examination was done. EDX results of the UPR before and after heated are tabulated in Table 1.

Table 1. EDX results of UPR before and after heated up to 80^{o}C

Element Symbol	**Before heated**		**After heated**	
	Atomic Concentration (%)	**Weight Concentration (%)**	**Atomic Concentration (%)**	**Weight Concentration (%)**
C	69.74	63.37	79.04	73.9
O	30.26	36.63	20.96	26.1

After heating, both the atomic and weight concentrations of carbon (C) have increased significantly, as show in Table 1. The atomic concentration and the weight concentration of carbon increased. Conversely, the concentrations of oxygen (O) have decreased after heating. The reduction in oxygen content could suggest a dehydration process, where water is driven off, or a reduction reaction, where oxygen is removed from the material (possibly forming a gas like CO or CO2 that escapes). The EDX analysis indicates that heating the material has significantly increased the carbon concentration while reducing the oxygen concentration. This suggests that the material undergoes a chemical transformation during heating, likely involving the loss of oxygen, possibly through the decomposition of oxides or the release of gaseous oxygen-containing species [35]. Decomposition typically leads to mass loss because lighter components, especially gases, escape from the material [36]. For durability characterization, the results show that the power loss value fluctuates as shown in Figure 7.

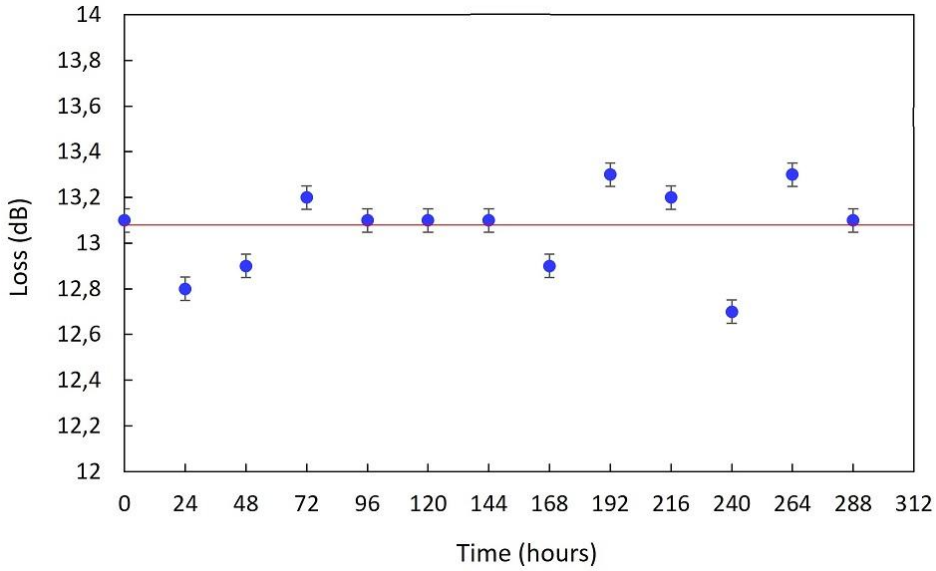


Figure 7. Power loss during long temperature exposure time at 40°C.

The standard deviation of power loss during long temperature exposure is 0.17 dB, as shown in Figure 7. The deviation occurred due to an error of the sensor system and heating device. It can be seen that there is no significant decrease in power loss after being exposed at 40°C for 288 hours. Therefore, it can be concluded that this waveguide can be applied for a long time at ambient temperature**.**

The obtained results confirm that the waveguide has good durability to thermal load. Although the result has quite small fluctuation resulted from the noise of the sensor system, the results also showed that it has a good thermal stability for application in temperature range of 25°C to 70°C. Therefore, the waveguide can be used for a long period under various environmental temperatures. However, if the waveguide is used for liquid refractive index sensor, temperature cross sensitivity should be considered since liquid refractive index is in the low range of 1.33 to 1.36 [37]. Due to the narrow range of refractive index, a slight refractive index measurement error leads to significant discrepancies in the realms of chemistry and biomolecules. Hence, temperature compensation technique should be carried out.

One primary limitation of the research is the environmental fluctuations affecting the accuracy of TDL characterization. This external temperature variation might have introduced errors in the measurements. To further improve the study, isolating the characterization setup to minimize these environmental influences is crucial. Additionally, future study could be carried out in exploring other materials with better thermal stability and lower temperature sensitivity to enhance the waveguide's performance. Implementing temperature compensation techniques is also recommended to improve the accuracy and reliability of the waveguide in precise applications, such as liquid refractive index sensing.

The findings from this research have significant implications in the field of Physics, particularly in the development and application of polymer-based optical waveguides. The study demonstrates that PMMA-based waveguides filled with UPR can maintain stable performance across a range of temperatures, making them suitable to be used in various environmental conditions. The findings are important for advancing low-cost and efficient optical sensing technologies. Through demonstrating the thermal durability and highlighting the limitations of the current waveguide design, this research sets the stage for future advancements in optical materials and waveguide fabrication techniques.

CONCLUSION

The research presented in this article explored the thermal durability of a simple optical waveguide fabricated using PMMA and UPR. The study has successfully characterized the TDL, temperature working range, and the long-term thermal exposure performance of the waveguide. It was observed that the power loss in the waveguide increases linearly with the temperature, with a TDL of 0.0235 dB/°C. This finding is significant as it quantifies the relationship between temperature and waveguide performance, which is crucial for practical applications where precise optical transmission is required. The waveguide was found to maintain its performance up to 70°C, beyond which significant degradation occurs, particularly noticeable at 80°C. This result determined a clear operational temperature range for the waveguide. Additionally, the long-term exposure tests at 40°C demonstrated that the waveguide showed stable performance over extended periods, confirming its potential for use in environments with fluctuating temperatures. In conclusion, the UPR-PMMA-based optical waveguide exhibits good thermal durability, maintaining stable performance up to a defined temperature threshold and during long-term thermal exposure. While there are some limitations related to environmental fluctuations, the overall findings showed the potential of these waveguides for cost-effective and reliable use in optical communication and sensing applications. The potential development of these findings for future research lies in the exploration of new materials and techniques to enhance the thermal stability and reduce the temperature sensitivity.

AUTHOR CONTRIBUTIONS

Ian Yulianti: Conceptualization, Methodology, Validation, Supervision, Writing-Original draft, Funding acquisiton; Shiva Maulana Khoiru Insan: Investigation, Visualization, Formal Analysis, Writing-Original Draft, Ngurah Made Darma Putra : Conceptualization, Formal Analysis, Writing- Review and Editing; Aji Purwinarko: Project administration, Data curation, Writing- Review and Editing; Nuni Widiarti : Project administration, Writing- Review and Editing; Nor Hafizah Ngajikin: Formal Analysis, Writing- Review and Editing**.**

DECLARATION OF COMPETING INTEREST

The authors declare that they have no known competing financial interests or personal relationships that could have appeared to influence the work reported in this paper.

REFERENCES

[1] Yulianti I, Ngurah Made DP, Lestiyanti Y, and Kurdi O. Optimization of Ridge Waveguide Structure for Temperature Sensor Application Using Finite Difference Method. *Proceeding of MATEC Web of Conferences*. 2018; **159**: 02020. DOI: https://doi.org/10.1051/matecconf/201815902020.

[2] He H-L, Li J, Zhang S-Y, Liu H, Ma J, Fan Y-X, et al. Multiplexing of Terahertz Signals Based on Gold-Coated Polymer Parallel-Plate Waveguides. *Optik (Stuttg).* 2023; **287**: 171113. DOI: https://doi.org/10.1016/j.ijleo.2023.171113.

[3] Liu C-Y. Fabrication and Optical Characteristics of Silicon-Based Two-Dimensional Wavelength Division Multiplexing Splitter with Photonic Crystal Directional Waveguide Couplers. *Physics Letter A*. 2011; **375**(28): 2754–2758. DOI: https://doi.org/10.1016/j.physleta.2011.06.017.

[4] Tian Y, Kang Z, He J, Zheng Z, Qiu J, Wu J, et al. Cascaded All-Optical Quantization Employing Step-Size MMI and Shape-Optimized Power Splitter. *Optics and Laser Technology*. 2023; **158**: 108820. DOI: https://doi.org/10.1016/j.optlastec.2022.108820.

[5] Chen Y, Chen Y, Lu M, Zhao Y, Hu G, Yun B, et al. Optimized Inverse Design of An Ultra-Compact Silicon-Based 2 × 2 3 dB Optical Power Splitter. *Optics Communications*. 2023; **530**: 129141. DOI: https://doi.org/10.1016/j.optcom.2022.129141.

[6] Serecunova S, Seyringer D, Uherek F, and Seyringer H. Waveguide Shape and Waveguide Core Size Optimization of Y-Branch Optical Splitters Up To 128 Splitting Ratio. *Optics Communications*. 2021; **501**: 127362. DOI: https://doi.org/10.1016/j.optcom.2021.127362.

[7] Wang Y, Wang KF, and Wang BL. Bending Mechanism of Optically Actuated All-Optical Mechanical Switches Composed of Bilayer Waveguides. *International Journal of Mechanical Sciences*. 2022; **222**: 107234. DOI: https://doi.org/10.1016/j.ijmecsci.2022.107234.

[8] ShangGuan L, Zhang D, Zhang T, Cheng R, Wang J, Wang C, et al. Functionalized Polymer Waveguide Optical Switching Devices Integrated with Visible Optical Amplifiers Based On An Organic Gain Material. *Dye Pigment*. 2020; **176**: 108210. DOI: https://doi.org/10.1016/j.dyepig.2020.108210.

[9] Jiang M, Zhang D, Lian T, Wang L, Niu D, Chen C, et al. On-Chip Integrated Optical Switch Based on Polymer Waveguides. *Optical Materials (Amst)*. 2019; **97**: 109386. DOI: https://doi.org/10.1016/j.optmat.2019.109386.

[10] Mamtmin G, Kari N, Abdurahman R, Nizamidin P, and Yimit A. 5, 10, 15, 20-Tetrakis-(4-Methoxyphenyl) Porphyrin Film/K+ Ion-Exchanged Optical Waveguide Gas Sensor. *Optics and Laser Technology*. 2020; **128**: 106260. DOI: https://doi.org/10.1016/j.optlastec.2020.106260.

[11] Mamtmin G, Nizamidin P, Abula R, and Yimit A. Composite Optical Waveguide Sensor Based on Porphyrin@ZnO Film for Sulfide-Gas Detection. *Chinese Journal of Analytical Chemistry*. 2023; **51**(7): 100260. DOI: https://doi.org/10.1016/j.cjac.2023.100260.

[12] Niu D, Zhang D, Wang L, Lian T, Jiang M, Sun X, et al. High-Resolution and Fast-Response Optical Waveguide Temperature Sensor Using Asymmetric Mach-Zehnder Interferometer Structure. *Sensors Actuators A: Physical*. 2019; **299**: 111615. DOI: https://doi.org/10.1016/j.sna.2019.111615.

[13] Malmir K, Habibiyan H, and Ghafoorifard H. Ultrasensitive Optical Biosensors Based on Microresonators with Bent Waveguides. *Optik (Stuttg)*. 2020; **216**: 164906. DOI: https://doi.org/10.1016/j.ijleo.2020.164906.

[14] Zhang H, Fan G, Cai X, Wei J, Jing G, Li S, et al. Quasi-Linear Response of An Integrated Optical Waveguide Sensor by A Double Output Readout Method. *Optik (Stuttg)*. 2021; **245**: 167734. DOI: https://doi.org/10.1016/j.ijleo.2021.167734.

[15] Ding Z, Wang H, Li T, Ouyang X, Shi Y, and Zhang AP. Fabrication of Polymer Optical Waveguides by Digital Ultraviolet Lithography. *Journal of Lightwave Technology*. 2022; **40**(1): 163–169. DOI: https://doi.org/10.1109/JLT.2021.3120712.

[16] Prajzler V, Chlupaty V, Kulha P, Neruda M, Kopp S, and Mühlberger M. Optical Polymer Waveguides Fabricated by Roll-to-Plate Nanoimprinting Technique. *Nanomaterials*. 2021; **11**(3): 724. DOI: https://doi.org/10.3390/nano11030724.

[17] Ishutkin SV, Arykov VS, Yunusov IV, Stepanenko M V, Troyan PE, and Zhidik YS. Development of Technology Formation of the Optical Waveguide Structures Based on InP by Plasma Etching. *Proceeding of 2019 20th International Conference of Young Specialists on Micro/Nanotechnologies and Electron Devices (EDM)*. 2019: 53–58. DOI: https://doi.org/10.1109/EDM.2019.8823278.

[18] Lv J, Hong B, Tan Y, Chen F, Rodríguez Vázquez de Aldana J, and Wang GP. Mid-Infrared Waveguiding in Three-Dimensional Microstructured Optical Waveguides Fabricated by Femtosecond-Laser Writing and Phosphoric Acid Etching. *Photonics Research*. 2020; **8**(3): 257–262. DOI: https://doi.org/10.1364/PRJ.380215.

[19] Lizarraga-Medina EG, Castillo GR, Jurado JA, Caballero-Espitia DL, Camacho-Lopez S, Contreras O, et al. Optical Waveguides Fabricated in Atomic Layer Deposited Al2O3 by Ultrafast Laser Ablation. *Results in Optics*. 2021; **2**: 100060. DOI: https://doi.org/10.1016/j.rio.2021.100060.

[20] Woods R, Feldbacher S, Langer G, Satzinger V, Schmidt V, and Kern W. Epoxy Silicone Based Matrix Materials for Two-Photon Patterning of Optical Waveguides. *Polymer (Guildf)*. 2011; **52**(14): 3031–3037. DOI: https://doi.org/10.1016/j.polymer.2011.04.052.

[21] Hamid H, Neeli M, Fickenscher T, O'Keefe SG, and Thiel DV. Simple Low-Cost Fabrication Method of A Buried Plastic Optical Waveguide for Circuits in Plastic Interconnects. *Microwave and Optical Technology Letters*. 2013; **55**(8): 1947–1950. DOI: https://doi.org/10.1002/mop.27683.

[22] Zheng L, Keppler N, Zhang H, Behrens P, and Roth B. Planar Polymer Optical Waveguide with Metal-Organic Framework Coating for Carbon Dioxide Sensing. *Advanced Material Technology*. 2022; **7**(12): 2200395. DOI: https://doi.org/10.1002/admt.202200395.

[23] Ryu JH, Lee TH, Cho I-K, Kim C-S, and Jeong MY. Simple Fabrication of A Double-Layer Multi-Channel Optical Waveguide Using Passive Alignment. *Optics Express*. 2011; **19**(2): 1183–1190. DOI: https://doi.org/10.1364/OE.19.001183.

[24] Yulianti I, Putra NMD, Astuti B, Kurniansyah KE, and Latif ZAF. Fabrication and Characterization of Polyester/Polymethylmethacrylate Buried Waveguide for Operation in Visible Light Range. *AIP Conference Proceedings*. 2019; **2169**: 060006. DOI: https://doi.org/10.1063/1.5132684.

[25] Yulianti I, Putra NMD, Fianti, Dewi AL, and Paradita D. Performances Characterization of Unsaturated Polyester Resin/Polymethylmethacrylate Waveguide for Refractive Index Measurement. *Optik (Stuttg)*. 2021; **242**: 167305. DOI: https://doi.org/10.1016/j.ijleo.2021.167305.

[26] Günther A, Baran M, Roth B, and Kowalsky W. Simulation and Experimental Verification of the Thermal Behaviour of Self-Written Waveguides. *Applied Sciences*. 2022; **11**(17): 7881. DOI: https://doi.org/10.3390/app11177881.

[27] Jing N, Teng C, Zheng J, Wang G, Zhang M, and Wang Z. Temperature Dependence of Light Power Propagation in Bending Plastic Optical Fiber. *Optical Fiber Technology*. 2016; **31**: 20–22. DOI: https://doi.org/10.1016/j.yofte.2016.05.006.

[28] Günther A, Baran M, Garg R, Roth B, Kowalsky W. Analysis of the thermal behavior of self-written waveguides. *Optics and Lasers Engineering*. 2022; **151**: 106922. DOI: https://doi.org/10.1016/j.optlaseng.2021.106922.

[29] Chencheni A, Belkhiri S, Tarchoun AF, Abdelaziz A, Bessa W, Boucheffa Y, and Trache D. Unravelling The Thermal Behavior and Kinetics of Unsaturated Polyester Resin Supplemented With Organo-Nanoclay. *RSC Advances.* 2024; **14**: 517-528. DOI: https://doi.org/10.1039/d3ra06076d.

[30] Salemane MG, Baruwa AD, and Makhatha ME. Investigating the Chemical Stability and Thermal Functionality of DMPT Promoted TiO2 Nanoparticles On Unsaturated Polyester Resin. *Results in Engineering.* 2024; **22**: 102116. DOI: https://doi.org/10.1016/j.rineng.2024.102116.

[31] Dai K, Song L, Jiang S, Yu B, Yang W, Yuen RKK, and Hu Y. Unsaturated Polyester Resins Modified With Phosphorus-Containing Groups: Effects on Thermal Properties and Flammability. *Polymer Degradation and Stability*. 2013; **98**(10): 2033-2040. DOI: https://doi.org/10.1016/j.polymdegradstab.2013.07.008.

[32] Dayan MAR, Habib MM, Uddin MM, Khatun M, Hossain MS, and Rashid MA. Characterization of Aloe Vera Gel Incorporated Unsaturated Polyester Resin Jute-Cotton

Fabric Composites for Enhanced Biodegradability, Flexibility, and Insulation Properties. *Heliyon*. 2024; **10**(15): e35261. DOI: https://doi.org/10.1016/j.heliyon.2024.e35261.

[33] Ren K and Tsai Y. Thermal Hazard Characteristics of Unsaturated Polyester Resin Mixed with Hardeners. *Polymers*. 2021; **13**(4): 522. DOI: https://doi.org/10.3390/polym13040522

[34] Dvořáčková Š and Kroisová D. Thermal Expansion of Composite System Epoxy Resin/Recycled Carbon Fibers. *Materials Science Forum*. 2020; **994**: 162–169. DOI: https://doi.org/10.4028/www.scientific.net/MSF.994.162.

[35] Salasinska K, Celiński M, Barczewski M, Leszczyński MK, Borucka M, and Kozikowski P. Fire Behavior of Flame Retarded Unsaturated Polyester Resin With High Nitrogen Content Additives. *Polymer Testing*. 2020; **84**: 106379. DOI: https://doi.org/10.1016/j.polymertesting.2020.106379.

[36] Halim ZAA, Yajid MAM, Nurhadi FA, Ahmad N, and Hamdan H. Effect of Silica Aerogel – Aluminium Trihydroxide Hybrid Filler On The Physio-Mechanical and Thermal Decomposition Behaviour of Unsaturated Polyester Resin Composite. *Polymer Degradation and Stability*. 2020; **182**: 109377. DOI: https://doi.org/10.1016/j.polymdegradstab.2020.109377.

[37] Li Y, Miao Y, Wang F, Wang J, Ma Z, Wang L, Di X, and Zhang K. Serial-Tilted-Tapered Fiber with High Sensitivity for Low Refractive Index. *Optics Express*. 2018; **26**(26): 34776-34788. DOI: https://doi.org/10.1364/OE.26.034776.